

OPEN ACCESS

EDITED BY

Benjamin R. Pittman-Polletta,
Boston University, United States

REVIEWED BY

Kelong Lu,
Wenzhou Medical University, China
Zhipeng He,
Sun Yat-sen University, China

*CORRESPONDENCE

Lilia Costa
✉ liliacosta@ufba.br

RECEIVED 26 December 2022

ACCEPTED 13 June 2023

PUBLISHED 27 July 2023

CITATION

do Nascimento DC, Santos da Silva JR, Ara A,
Sato JR and Costa L (2023) Hyperscanning
fNIRS data analysis using multiregression
dynamic models: an illustration in a violin duo.
Front. Comput. Neurosci. 17:1132160.
doi: 10.3389/fncom.2023.1132160

COPYRIGHT

© 2023 do Nascimento, Santos da Silva, Ara,
Sato and Costa. This is an open-access article
distributed under the terms of the [Creative
Commons Attribution License \(CC BY\)](#). The use,
distribution or reproduction in other forums is
permitted, provided the original author(s) and
the copyright owner(s) are credited and that
the original publication in this journal is cited, in
accordance with accepted academic practice.
No use, distribution or reproduction is
permitted which does not comply with these
terms.

Hyperscanning fNIRS data analysis using multiregression dynamic models: an illustration in a violin duo

Diego Carvalho do Nascimento¹, José Roberto Santos da Silva^{2,3},
Anderson Ara⁴, João Ricardo Sato⁵ and Lilia Costa^{2*}

¹Departamento de Matemática, Facultad de Ingeniería, Universidad de Atacama, Copiapó, Chile,

²Department of Statistics, Federal University of Bahia, Salvador, Brazil, ³EcMetrics Pesquisa de Mercado, Salvador, Brazil, ⁴Departamento de Estatística, Universidade Federal do Paraná, Curitiba, Brazil, ⁵Center of Mathematics, Computing and Cognition, Universidade Federal do ABC, São Bernardo do Campo, Brazil

Introduction: Interpersonal neural synchronization (INS) demands a greater understanding of a brain's influence on others. Therefore, brain synchronization is an even more complex system than intrasubject brain connectivity and must be investigated. There is a need to develop novel methods for statistical inference in this context.

Methods: In this study, motivated by the analysis of fNIRS hyperscanning data, which measure the activity of multiple brains simultaneously, we propose a two-step network estimation: Tabu search local method and global maximization in the selected subgroup [partial conditional directed acyclic graph (DAG) + multiregression dynamic model]. We illustrate this approach in a dataset of two individuals who are playing the violin together.

Results: This study contributes new tools to the social neuroscience field, which may provide new perspectives about intersubject interactions. Our proposed approach estimates the best probabilistic network representation, in addition to providing access to the time-varying parameters, which may be helpful in understanding the brain-to-brain association of these two players.

Discussion: The illustration of the violin duo highlights the time-evolving changes in the brain activation of an individual influencing the other one through a data-driven analysis. We confirmed that one player was leading the other given the ROI causal relation toward the other player.

KEYWORDS

dynamic network, state-space models, causal inference, dual brain, interactive social neuroscience

1. Introduction

The brain is formed by a network in which different regions share information [Horwitz \(2003\)](#). This brain network can be studied through *functional connectivity*, which represents the patterns of statistical dependence on the activity of distinct brain regions, or through *effective connectivity*, which means the causal influences of the activity of one region over another. The variance-covariance matrix and the Bayesian network (BN) are examples of methods used to estimate functional connectivity. Other methods can be used to study effective connectivity, such as dynamic causal modeling (DCM) and the multiregression dynamic model (MDM). For a given directed network structure, the MDM models the data at each node as a linear combination of the parent nodes with time-varying connectivity parameters. According to [Queen and Smith \(1993\)](#), the MDM can distinguish between directed graphs corresponding to the same statistical dependence structure (which map onto

the same undirected graphs), allowing for the accurate estimation of the directions of edges (a simple example of this is also discussed here). Moreover, the MDM can be observed as more than a static network (similar to BN). Alternative examples of these dynamic methods can be found in [Burger et al. \(2009\)](#), who used the dynamic Bayesian network (DBN) and hidden Markov models (HMM) used in human-robot interaction (DBN and HMM are a particular case of MDM).

In any case, the problem of finding a common pattern of brain connectivity for a given individual profile (healthy or with a specific disease, e.g., Alzheimer's disease) is not trivial owing to the presence of noise and the high-dimensionality of the data ([Nascimento et al., 2020](#); [Pinto-Orellana et al., 2020](#)). For the MDM, [Costa et al. \(2015\)](#) presented a score-based learning network approach using a linear programming problem that finds the most likely network structure while considering the subset comparison through their maximum posterior probability (MAP) estimation. The authors demonstrated the usefulness of their method on functional Magnetic Resonance Imaging (fMRI) data as it becomes unfeasible as the number of nodes (i.e., brain regions) increases.

In addition to this challenge, in the field of social neuroscience, understanding how the activity of the brain might influence the activity of another brain, which is known as brain-to-brain activity correlation, is also desirable. As examples, we considered a classroom where the teacher and the students interact or an orchestra where the musicians and the conductor interact. [Konvalinka and Roepstorff \(2012\)](#) describes how mutually interacting brains can be useful in social interaction. [Balconi et al. \(2017\)](#) studied the effects of strategic cooperation on intra- and inter-brain connectivity by functional near-infrared spectroscopy (fNIRS). [Jiang et al. \(2019\)](#) developed a study entitled "BrainNet: a multi-person brain-brain interface for direct collaboration between brains," among others.

Hyperscanning studies—measuring the activity of multiple brains simultaneously—is a promising (flexible) paradigm regarding the measurement of brain activity from two or more people simultaneously while they are interacting. This could reveal interpersonal brain mechanisms underlying interaction-mediated brain-to-brain coupling [Scholkmann et al. \(2013\)](#). One experiment that could be conducted to this end, focusing on two brains' observations, is the study of violin duos playing together. The fNIRS could be used to overcome functional magnetic resonance imaging constraints, but few dynamic data-driven models have been proposed. Thus, we aimed to apply a dynamic graphical model to show dynamic changes in intersubject brain activity dependence over time.

1.1. Interaction-mediated brain-to-brain activity correlation

In recent decades, part of the neuroscience field has focused on demonstrating the nervous system and its function through individuals' behavior (and inter-relations) ([Liu and Pelowski, 2014](#)). For instance, some studies have discussed the brain connectivity structure by gender ([Wang et al., 2009](#); [Baker et al., 2016](#); [Pan et al.,](#)

[2017](#)), age ([Gong et al., 2009](#)), or using other characteristics such as intelligence ([Song et al., 2008](#); [Van Den Heuvel M. et al., 2008](#); [van den Heuvel M. P. et al., 2008](#)), psychoactive ingestion ([Palhano-Fontes et al., 2019](#)), and meditative states ([Brefczynski-Lewis et al., 2007](#); [Brewer et al., 2011](#); [Hasenkamp and Barsalou, 2012](#)). Nevertheless, all of them have targeted different methodologies related to neuroanatomy. These methodologies also understand the brain connection patterns in human actions, such as opening and closing eyes (or moving any other body part), reading, writing, playing sports, learning, sleeping, creating memories, and recalling these memories ([Hahn et al., 2018](#)).

However interpersonal neural synchronization (INS) demands a greater understanding of the influence that a brain may carry on others rather than observing only a single brain response per time (for further details, see [Babiloni and Astolfi, 2014](#)). Hyperscanning studies are based on the simultaneous acquisition of brain dynamics during a cooperative task, as a joint action or decision-making ([Liu et al., 2016, 2017](#)).

[Li et al. \(2020\)](#) studied the cooperative behavior among basketball players, in which significant INS was observed due to the performed joint-drawing task but not the control task. [Nguyen et al. \(2020\)](#) investigated the neural processes related to transferring information across brains during naturalistic teaching and learning, underlying the effective communication of complex information across brains in classroom settings.

With more than only linking actions across subjects, studies have revealed that inter-individuals' neural representation can even build memories, thereby promoting brain integration at some influential level. [Zadbood et al. \(2017\)](#) uncovered the intimate correspondences between memory encoding and event construction and highlighted the essential role that our common language plays in the process of transmitting one's memories to other brains. [Chen et al. \(2017\)](#) elucidated that the neural patterns during perception are systematically altered across people into shared memory representations for real-life events.

Most methods used in hyperscanning fMRI and fNIRS studies are static or temporal correlation ([Cui et al., 2012](#); [Reindl et al., 2022](#); [Balconi and Angioletti, 2023](#); [Morgan et al., 2023](#); [Wei et al., 2023](#)) and Granger-based causality ([Zhang et al., 2017](#); [Chen et al., 2020, 2023](#); [Pan et al., 2021](#); [Zhao et al., 2022](#)). Examples of the former method are the partial correlation coefficient and wavelet transform coherence (WTC). These methods are used to estimate functional connectivity and, therefore, do not distinguish the causal relationships between nodes. Nonetheless, according to neuroimaging literature, the latter is used to estimate directed functional connectivity ([Bilek et al., 2022](#)), and according to some studies, Granger causality theory cannot be suitable for hemodynamic data ([Smith et al., 2011](#); [Babiloni and Astolfi, 2014](#)). Therefore, these approaches do not study putative causal synchrony between brains ([Bilek et al., 2022](#)). Thus, [Bilek et al. \(2022\)](#) used dynamic causal modeling (DCM) in the study of social interaction to estimate the causal effect one brain might have on another. However, DCM is a method for testing hypotheses, and initially specifying some candidate network structures is necessary.

This study uses the MDM with the Bayes factor (MDM-BF) that considers the contemporaneous relationship between regions, i.e., the nodes are related at the same time, in contrast, for example,

to a DBN in which the past of the parents is connected with the present of the child. Moreover, the Kalman filtering method is used to estimate the effective connectivity in a simple way. However, in contrast to DCM, it can capture the dynamic nature of social interaction. A similar objective can be observed in Li et al. (2021) and Wang et al. (2022), in which the researchers used a data-driven approach based on sliding windows and k -mean clustering to capture the dynamic modulation of inter-brain synchrony patterns. However, it is based on temporal correlation and does not estimate effective connectivity.

The MDM appears to accommodate fMRI data well (see e.g., Costa et al., 2015); therefore, it has been used in this study for the first time with fNIRS data. Furthermore, this study proposes a new method that can be used to learn the directed acyclic graph (DAG) structure using the MDM faster than the method already available in the literature (MDM-IPA) because this method does not create the need to check all possible parents for each node. This can be especially useful in social neuroscience—which involves estimating both inter-brain and intra-brain connections and thus studying brain function on the subject and dyadic levels.

This novel method consists of two steps: in the first one, the tabu search algorithm would be applied to find a partial conditional directed acyclic graph (partial conditional DAG). The tabu search is a combinatorial optimization algorithm used to find an optimal network structure by local searches, as explained in the next section. Then, the Markov equivalence class would be found, that is, DAGs that encode the same statistical properties, and the DAG with the highest log predictive likelihood (LPL) score from the MDM would be chosen. This search method can also be used to estimate individual brain networks.

Based on such evidence, which highlights the possibility of studying the brain-to-brain activity correlation, in the next subsection, we have discussed an extension class of DBNs that can be used to represent these brain dynamic and causal structures (from now on, whenever we refer to causality, it is associated with effective connectivity via MDM-BF, unless indicated differently).

This study is divided into four parts. In Section 2, we have described the fNIRS data analyzed and the methods used to estimate brain connectivity as a graph-based model. Section 3 describes the evaluation, through synthetic data, of the robustness of the dynamic graphical model. Then, Section 4 presents the empirical results, and finally, Section 5 presents the discussion of the proposed method and the findings.

2. Materials and methods

We present a proof-of-concept based on a hyperscanning experiment in which the human interaction is investigated from brain-to-brain activity dependence. The methodological approach adopted in this study was divided into four main steps, aiming to estimate the brain's dynamics and interactions. The developed R script in this study is available at <https://github.com/ProfNascimento/MDM-BF> (accessed on April 20th, 2023).

2.1. The data

This study dataset was first presented as a case study experiment (Balardin et al., 2017) that considered two individuals who played in a violin duo. In the current study, we have investigated the brain-to-brain coupling (and the direction) and explored which brain regions of a violinist are linked to the other.

The fNIRS signals acquired are demonstrated in Figure 1 (for further experiment details, see Balardin et al., 2017). Hemodynamic changes were obtained from the optical changes collected using the continuous wave functional near-infrared spectroscopy system (NIRScout 16x16, NIRx Medical Technologies, Glen Head, NY) with 16 LED light sources (760 and 850 nm) and 16 detectors per musician, at a sampling rate of 7.81 Hz. Channel aggregation was conducted by considering the EEG 10-10 system in which the optodes were placed.

The participants were at a professional level, right-handed, and men aged 41 and 50 years old. They were instructed to play a 32-s stretch of Allegro, by Antonio Vivaldi, from Concerto No 1 in E major, op. 8, RV 269, "Spring." Hyperscanning was performed considering 23 channels of the right motor hemisphere and the temporoparietal junction of the two violinists (Balardin et al., 2017). The first 36 s of acquisition refers to the duo playing and the remaining refers to a resting-state condition.

2.2. Dataflow

Figure 2 demonstrates a data processing flow chart. Given the computational cost of searching for the likely topology of the graph, at first, the tabu search algorithm was applied using Bayesian networks to reduce the sub-graph structure to be sought. Then, the result was transformed into a partial conditional directed acyclic graph (DAG), enabling it to proceed under the causal inference paradigm (Pearl, 2009; Oates et al., 2015). After that, the most likely undirected network structure found was implied in Markov equivalent graphs, and then, the MDM was applied to unravel directionality through the maximization of the LPL, that is, Bayes factor. By adopting a particle filter supposing Gaussian noises (often known as the Kalman filter), we compared the MAP graphs to obtain the most likely DAG. Once the DAG is defined, the MDM-BF can present the dynamic strength of these estimated links. This adopted methodology enables the estimation of complex brain structures whenever the number of vertices (nodes) is >11 with a sample size > 100 points (for further details, see Costa et al., 2015, Table 01, p. 456), without computational constraints.

2.3. The multiregression dynamic model

The MDM models multivariate time series, studying putative causal relations among its variables over time (Queen and Smith, 1993; Queen and Albers, 2009). This class of models is extremely powerful, given that it can discriminate complex multivariate relations up to a finite r -th time series, with length t , set as $(Y_t(1), Y_t(2), \dots, Y_t(r))$. Moreover, the joint distribution $(P(Y_t(1), Y_t(2), \dots, Y_t(r)))$ is estimated regardless of the presence

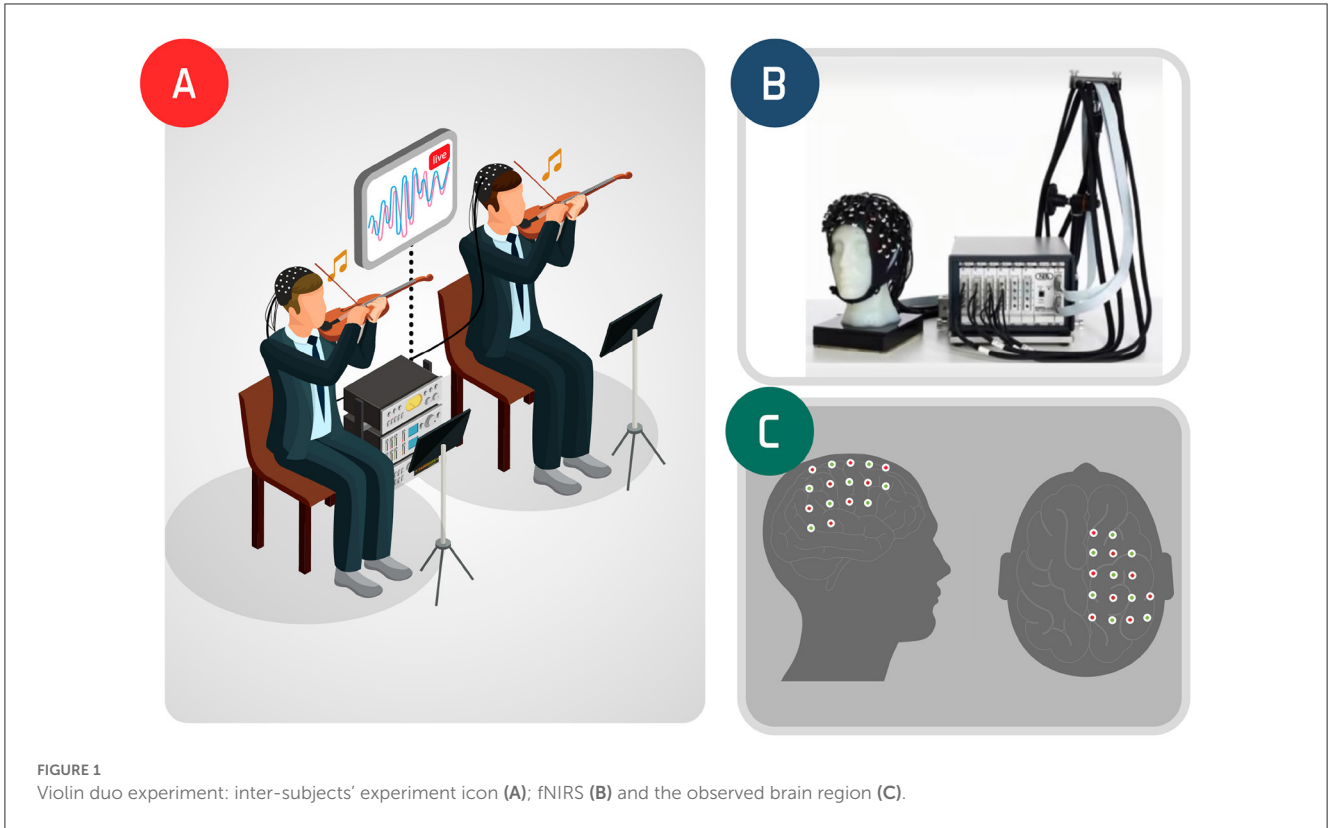


FIGURE 1 Violin duo experiment: inter-subjects' experiment icon (A); fNIRS (B) and the observed brain region (C).

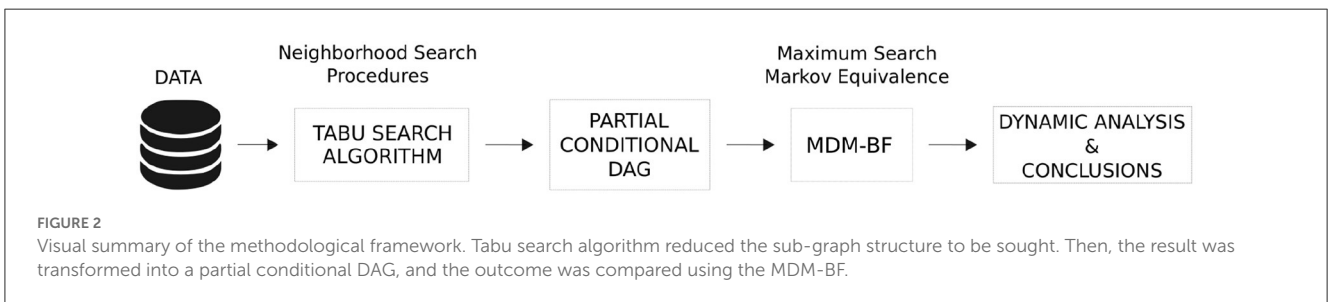


FIGURE 2 Visual summary of the methodological framework. Tabu search algorithm reduced the sub-graph structure to be sought. Then, the result was transformed into a partial conditional DAG, and the outcome was compared using the MDM-BF.

of a Gaussianity (for further details, please see [Queen and Smith, 1993](#), who have retained the proof of the consistency of this method of non-Gaussian processes). The MDM is formed by using univariate regression dynamic linear models (DLMs), in which the observation $Y_t(r)$ is regressed onto its parents, with Gaussian residuals, such as in Equation (1).

$$\begin{aligned}
 Y_t(r) &\sim \mathcal{N}(\mathbf{F}_t(r)' \boldsymbol{\theta}_t(r), V_t(r)) \\
 \boldsymbol{\theta}_t &\sim \mathcal{N}(\mathbf{G}_t \boldsymbol{\theta}_{t-1}, \mathbf{W}_t),
 \end{aligned}
 \tag{1}$$

where $Y_t(r)$ is an observable variable at time t and brain region r , $r = 1, \dots, n$ regions, $t = 1, \dots, T$ time points, \mathcal{N} denotes the Gaussian distribution, $\boldsymbol{\theta}'_t = (\boldsymbol{\theta}_t(1)', \dots, \boldsymbol{\theta}_t(n)')$, $\boldsymbol{\theta}_t(r)'$ is the p_r -dimensional parameter vector for $Y_t(r)$, and, when it is not intercepted, it represents the effective connectivity between node r and its descendant (also called parents). $\mathbf{F}_t(r)$ is the set of the parents, and for nodes that do not have parents, $\mathbf{F}_t(r) = \mathbf{1}$. \mathbf{G}_t increments the state equation in the form, giving extra variance.

In addition, $\mathbf{W}_t(r)$ are p_r square matrices that form $\mathbf{W}_t = \text{blockdiag}\{\mathbf{W}_t(1), \dots, \mathbf{W}_t(n)\}$. Note that, when $\mathbf{W}_t(r)$ is a matrix with all elements equal to zero, the MDM becomes the BN. The parameters can be estimated using well-known Kalman filter recurrences over time (see, for example, [West and Harrison, 2006](#)). By so doing, the DLM is described by the set $\{\mathbf{F}_t(r), V_t, \mathbf{G}_t, \mathbf{W}_t\}$, although, in practice, establishing the \mathbf{W}_t is challenging; therefore, a strategy called “discounting” (stochastic shifting) is adopted.

$$\mathbf{W}_t = \frac{1 - \delta}{\delta} \times \mathbf{C}_{t-1},
 \tag{2}$$

where \mathbf{W}_t is specified directly through a discount factor $\delta \in (0, 1]$, and \mathbf{C}_{t-1} is the posterior variance of $\boldsymbol{\theta}_t$.

Before proceeding, three terminologies are important for distinguishing estimation processes: (i) Filtering is a procedure that aims to update the current estimates as new data are observed, i.e., $\mathbb{P}(\boldsymbol{\theta}_t | Y_{1:t})$; (ii) smoothing is a retrospective analysis that has all the observations and calculates the conditional distribution $\boldsymbol{\theta}$ given the

heading from the complete data, $\mathbb{P}(\theta_t | Y_{1:T})$; and (iii) prediction is a forecast procedure that estimates the next observation based on the distribution, $\mathbb{P}(\theta_{t+1} | Y_{1:t})$.

2.4. The proposed learning network

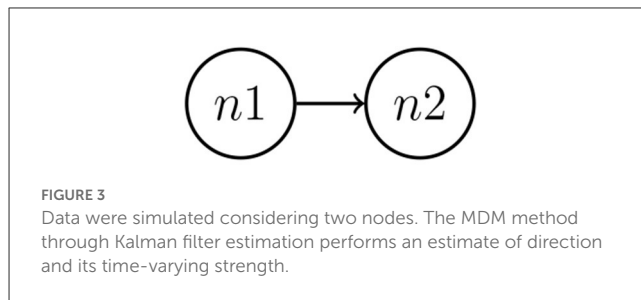
The learning network process used in this study is 2-fold: (i) an estimation process of a Bayesian network structure, the tabu search algorithm, and (ii) choosing a structure via the MDM in Markov equivalent networks, that is, partial conditional DAG \rightarrow MDM-BF. This methodological combination is an alternative to reduce the np-hard (dimensional) complexity search problem of the network estimation.

First, the initial estimation process is related to traditional methods in Bayesian networks (time-invariant structure). This approach was performed using a score-based method via standard tabu search with Bayesian information criterion (BIC). In general, this method searches for a Bayesian network structure that maximizes BIC. A Tabu search (Glover, 1986) may be viewed as a meta-heuristic algorithm to perform a greedy search and to avoid local minima. Thus, the procedure records information about changes recently made in BN structures, using one or more tabu lists. The tabu lists are managed by recording moves in a sequential order. Each time a new link is added to the end of a list, the oldest arc on the list is dropped from the beginning. Thus, each structure generated by adding or removing links is appraised by the BIC scoring (Nagarajan et al., 2013). The tabu algorithm adopted here can be found in the bnlearn package from the R software (R Core Team, 2022). Furthermore, every statistical analysis used in this study adopted the software R.

As it is well known that the BN search approaches have trouble distinguishing Markov equivalent structures, the next step was to find the graphs that are Markov equivalent to one resulting from the tabu search. Afterward, the network structure with the largest score of MDM among these Markov equivalent graphs was chosen. The pcalg package was used to obtain the partial conditional DAG.

Once the partial DAG structure was established, only a few subsets of possibilities remain to be sought. At this point, the maximum likelihood approach was adopted to determine the best options for the subgroup. The assumption from the MDM is that the standardized conditional one-step forecast errors have an approximate Gaussian distribution, although not based on stationary time series, and are serially independent with constant variance. Under these assumptions, the joint log predictive likelihood (LPL) has the closed form of a noncentral t distribution and is easily found in the Kalman filter (Costa et al., 2015). Remembering that $\mathbb{Y} = \{Y_t(1), \dots, Y_t(r)\}$ if time-invariant $\mathbb{Y} = \{Y(1), \dots, Y(r)\}$, considering a multivariate non-central t distribution function

$$f(\mathbb{Y}|\mu, \sigma^2\Sigma, \nu) = \frac{\Gamma[(\nu + r)/2]}{(\pi\nu)^{r/2}|\sigma^2\Sigma|^{1/2}\Gamma[\nu/2]} \left(1 + \frac{(\mathbb{Y} - \mu)' \Sigma^{-1} (\mathbb{Y} - \mu)}{\sigma^2\nu}\right)^{-(\nu+r)/2} \tag{3}$$



in which μ is the vector of the means and Σ is the variance-covariance matrix under the Bayesian framework

$$\mathbb{P}(\tau, \mathbb{Y}|\mu, \sigma^2\Sigma, \nu) \propto \mathbb{P}(\mathbb{Y}|\tau, \mu, \sigma^2\Sigma)\mathbb{P}(\tau|\nu) \tag{4}$$

$$\mathbb{Y}|\tau, \mu, \sigma^2\Sigma \sim N(\mu, (\sigma^2\Sigma/\tau)) \tag{5}$$

$$\tau|\nu \sim Ga(\nu/2, \nu/2) \tag{6}$$

and then assuming that the conditional distribution of each $Y_t(r)$ is given by the previous information set \mathcal{F}_{t-1} , one can simply consider a regression structure for the conditional mean $\mu_t = \mathbf{F}_t(r)' \theta_t(r)$ and $\Sigma_t = V_t$

$$\begin{aligned} \log(f(Y_t(1), \dots, Y_t(r)|\mathcal{F}_{t-1})) &= \log(L(\mathbf{F}_t(r)' \theta_t(r), V_t|\mathcal{F}_{t-1})) \\ &= LPL(\mathbf{F}_t(r)' \theta_t(r), V_t|\mathcal{F}_{t-1}) \end{aligned} \tag{7}$$

Therefore, the LPL is the score of the MDM used in the learning network process, and in the following section, Section 3, a simple example of the ability of this score to distinguish two Markov equivalent graphs is given. It must be mentioned that local Gaussian models do not imply, necessarily, a posterior symmetrical multivariate distribution (for further details, see Queen and Smith, 1993).

3. Simulating the MDM

This simulation study aimed to present the performance of the MDM in estimating the network structure and relationship strength (parameter θ) between the two nodes over time. Each time series contains 300 observations, that is, $t = \{1, \dots, 300\}$. Figure 3 represents the theoretical (known) network, in which node 1 (n1) is the parent of node 2 (n2). The data simulation was performed by using R software.

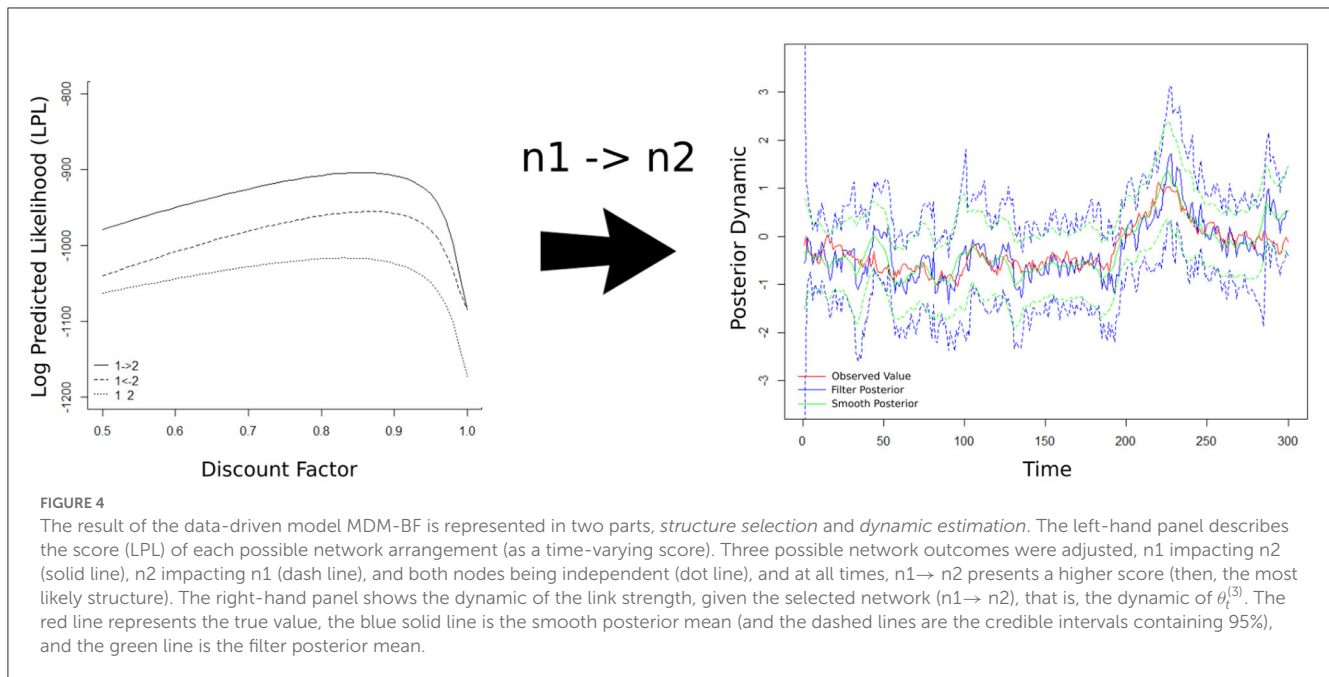
For instance, let us suppose that two signals, $n1(t)$ and $n2(t)$, are related, and they can be written as a first-order linear-Gaussian state-space model (these models presenting Gaussian noises are often called the Kalman filter, which is a special case of a particle filter for contemporaneous influence), as demonstrated in the following equations:

$$n1_t = \theta_t^{(1)} + v_t^{(1)}, v_t^{(1)} \sim \mathcal{N}(0, 0.1^2) \tag{8}$$

$$n2_t = \theta_t^{(2)} + \theta_t^{(3)} n1_t + v_t^{(2)}, v_t^{(2)} \sim \mathcal{N}(0, 0.1^2), \tag{9}$$

$$\theta_t^{(k)} = \theta_{t-1}^{(k)} + w_t^{(k)}, w_t^{(k)} \sim \mathcal{N}(0, 0.1^2) \tag{10}$$

in which $k = \{1, 2, 3\}$, and $v^{(1)}$, $v^{(2)}$, and $w^{(k)}$ are independent. There are structural equations containing time-varying parameters



$\theta_t^{(1)}$, $\theta_t^{(2)}$, and $\theta_t^{(3)}$. The parameters $\theta_t^{(1)}$ and $\theta_t^{(2)}$ are the drift that translates the strength for each node i at time t . The parameter $\theta_t^{(3)}$ is assumed to represent the form of the exchangeable sample information, in which (n1) impacts into (n2), and then, later, this is observed as a causal strength (in neuroscience, the effective neuronal connectivity).

After generating and processing the synthetic network, the left-hand panel of **Figure 4** shows the estimated LPL for each possible network set (that is, $n1 \rightarrow n2$, $n2 \rightarrow n1$, and both independent nodes) by a discount factor (DF). In the inference process of the MDM-BF, $W_t^{(r)}$ can be written in the function of a DF that represents the loss of information in the change of parameter θ between times $t - 1$ and t . The DF varies between zero and one, in a way that the closer the DF is to one, the more stable the system is. When DF assumes the value one, $W_t^{(r)}$ is the matrix of zeros, and the MDM becomes a BN (Costa et al., 2015). After selecting the most likely model, the strength dynamism of the connection is calculated through a time-varying parameter (θ_t) approach. The right-hand panel of **Figure 4** shows the true value and the MDM dynamic estimation regarding the causal effect between the nodes.

The steps are summarized in **Algorithm 1** summarized as follows:

In this case, the network with the highest LPL values was network $n1 \rightarrow n2$, which generated the data. Markov equivalent networks have the same dependency relations between the nodes and have equivalent/equal LPL. Therefore, when the discount factor is 1, as we mentioned, there is no variation in the state parameters over time, and the MDM simply becomes a BN. Then, unsurprisingly, the direction $n1 \rightarrow n2$ or $n2 \rightarrow n1$ does not matter (see the left-hand panel of **Figure 4**). Thus, this study presents an indication that the MDM-BF is efficient in distinguishing structures that can be Markov equivalent. Here, we described the simplest case of a network

Read the DATA

Apply the TABU search using the Bayesian Network to estimate the invariant structure

if $n1 \rightarrow n2$ or $n2 \rightarrow n1$ **then**

$n1, n2$ are independent

else

$n1 \rightarrow n2$ or $n2 \rightarrow n1$

Then, $n1$ is connected to $n2$ but partial conditional, that is, the direction will be ignored at this point. For a greater number of nodes, every combination will be tested.

end if

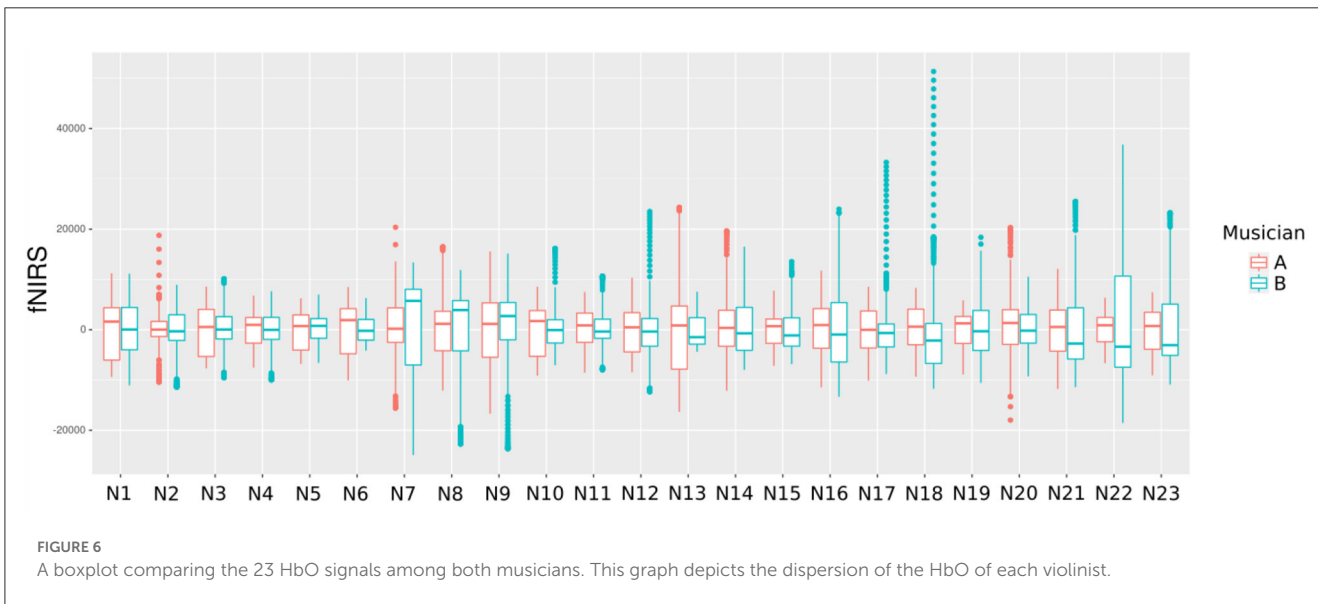
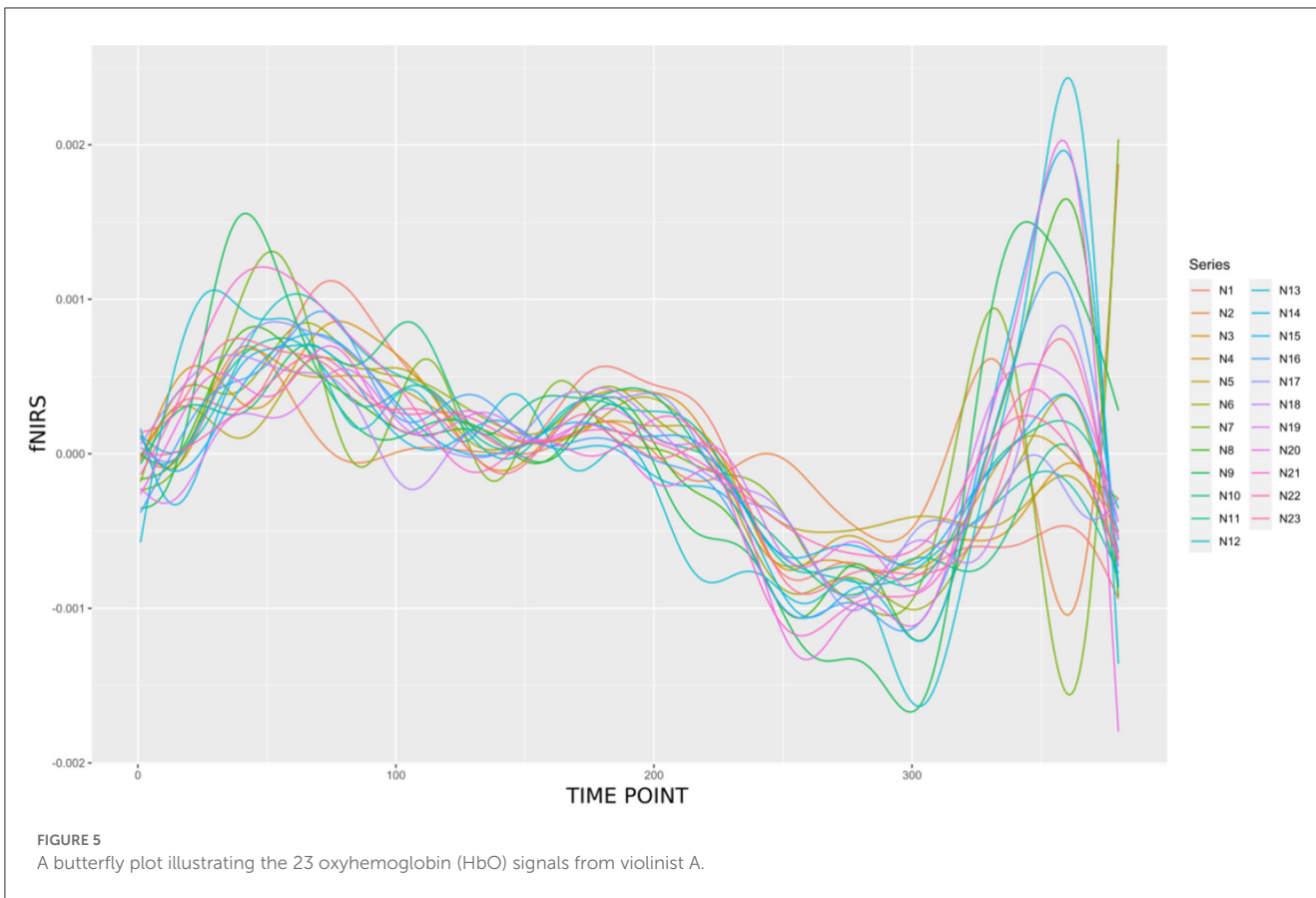
Calculate LPL from the TABU search subgroup, the partial conditional DAG ($n1 \rightarrow n2$ or $n2 \rightarrow n1$).

Then, the choice will be the DAG with the maximum LPL (that is, the directions that are established).

Once the DAG is set, the dynamic linear model is adjusted on the DAG regression structure (time-varying parameters estimation step, that is MDM-BF).

Algorithm 1. Causal inference MDM-BF schematic (based on **Figure 2**).

structure (with only two nodes) for the sake of simplicity and visualization; nevertheless, the results are expandable to higher complexities (see e.g., in Costa et al., 2015). The next section discusses the results obtained in neuroscience application tasks.

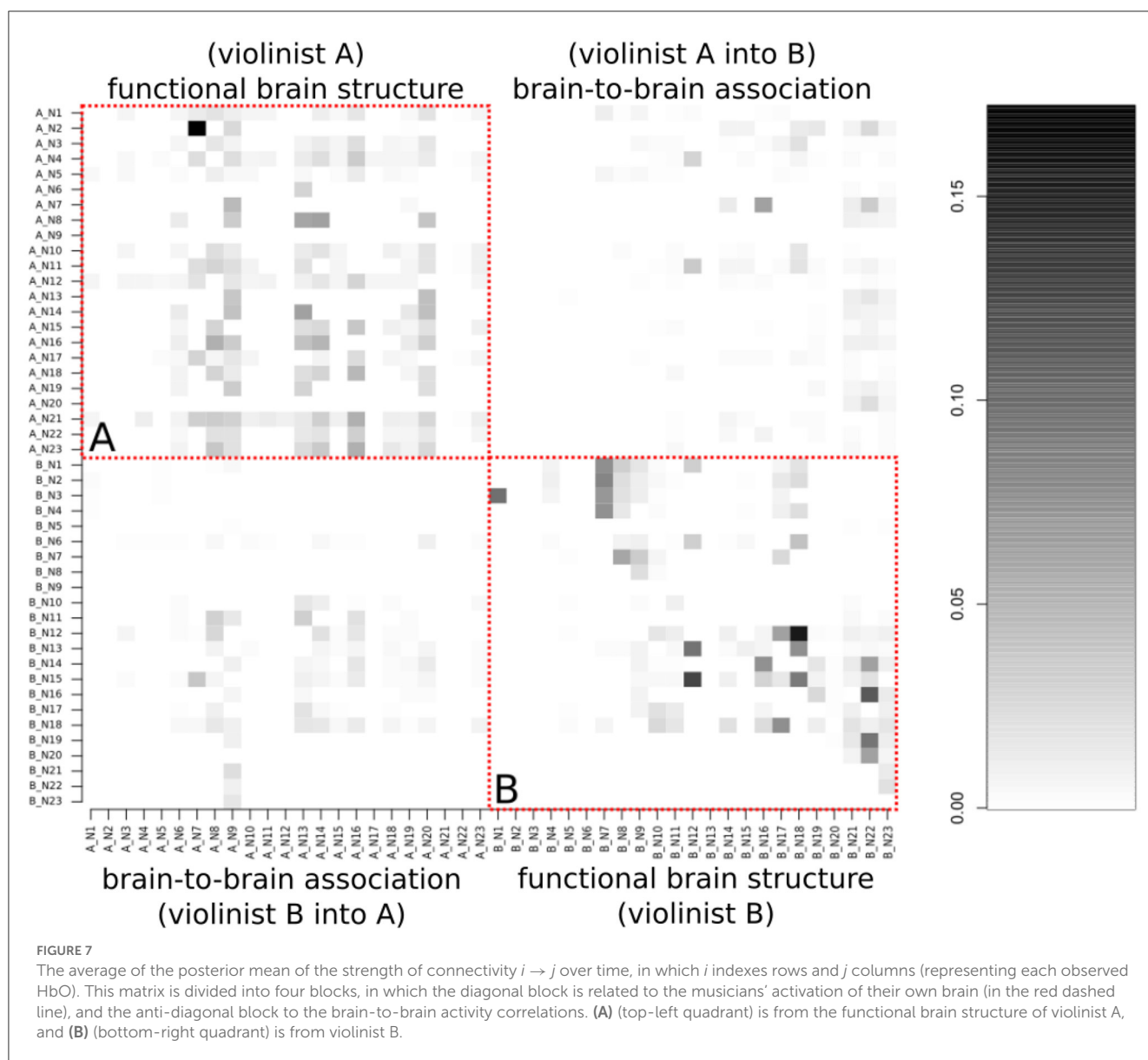


4. Experimental results

fNIRS enables simultaneous recording, making it possible to study the influence of brain-to-brain coupling through social interaction experiments. **Figure 5** shows the fNIRS data during the music duration (218 time points) from violinist A in the 23 channels.

4.1. Dynamic brain-to-brain evolution

The study of the network involved the brains of the two violinists and considered 46 nodes, the first 23 ones corresponding to the first subject, and the remaining ones to the second subject (**Figure 6**). The learning of the network structure was carried out by comparing the Markov equivalent networks to the graph



estimated by the tabu method and using the LPL of the MDM. The combination of the tabu search algorithm, partial conditional DAG, and the MDM-BF helped enhance the computation efficiency, bringing back the best network structure chosen for each subject.

The brain activation dynamic was analyzed by using the state-space model, obtained from the MDM-BF through its posterior mean smoothing process. It is worth mentioning that only positive connections (ignoring the few small negative estimates, as physiological interpretations are difficult to make) were presented, which enabled us to take into account their neurological interpretability. Moreover, these connections represent the neural activation resulting from one region's influences over another.

Figure 7 presents the results of the graph-based MDM, as a matrix in which each element is the average of the posterior mean of the strength of connectivity $i \rightarrow j$ over time, in which i (parents) indexes rows and j (children) indexes columns (the matrix causal relation direction is described from the row to the column).

Moreover, this matrix is divided into four blocks, in which the diagonal block is intrasubject connectivity, for violinist A, at the top left square and for violinist B, at the lower right square. In contrast, the anti-diagonal block shows intersubject connectivity, in which the influence of the brain regions of violinist A to B is at the top right, whereas the influence of violinist B to A is at the lower left.

Stronger connections are represented in the matrix by the darker color, while lighter regions represent weak or absent connections. As expected, the strongest connections are in the primarily diagonal block, which represents the intrasubject brain connections. The anti-diagonal block reveals that the intersubject connectivities are less prevalent and less strong. Thus, based on a standard 10-10 EEG montage, we aggregated the channel numbers 1, 2, 3, and 4 as dorsal frontal Regions of Interest (ROIs) 6, 7, 8, 10, and 11 as sensorimotor ROIs, and 12, 13, 15, 16, and 21 as temporoparietal junction (TPJ) and calculated the mean of the influence of each region. A summary of the intra-individual

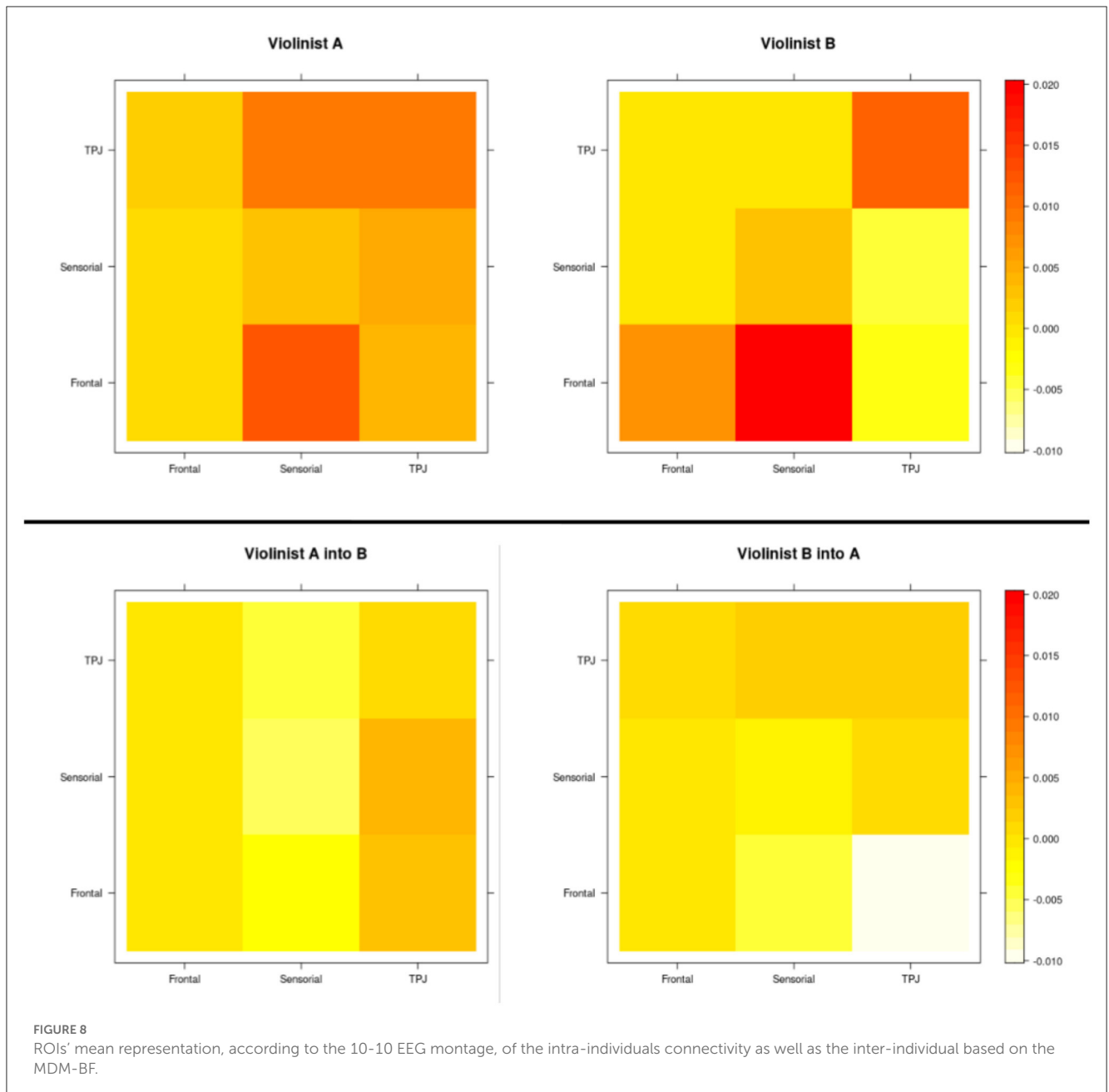


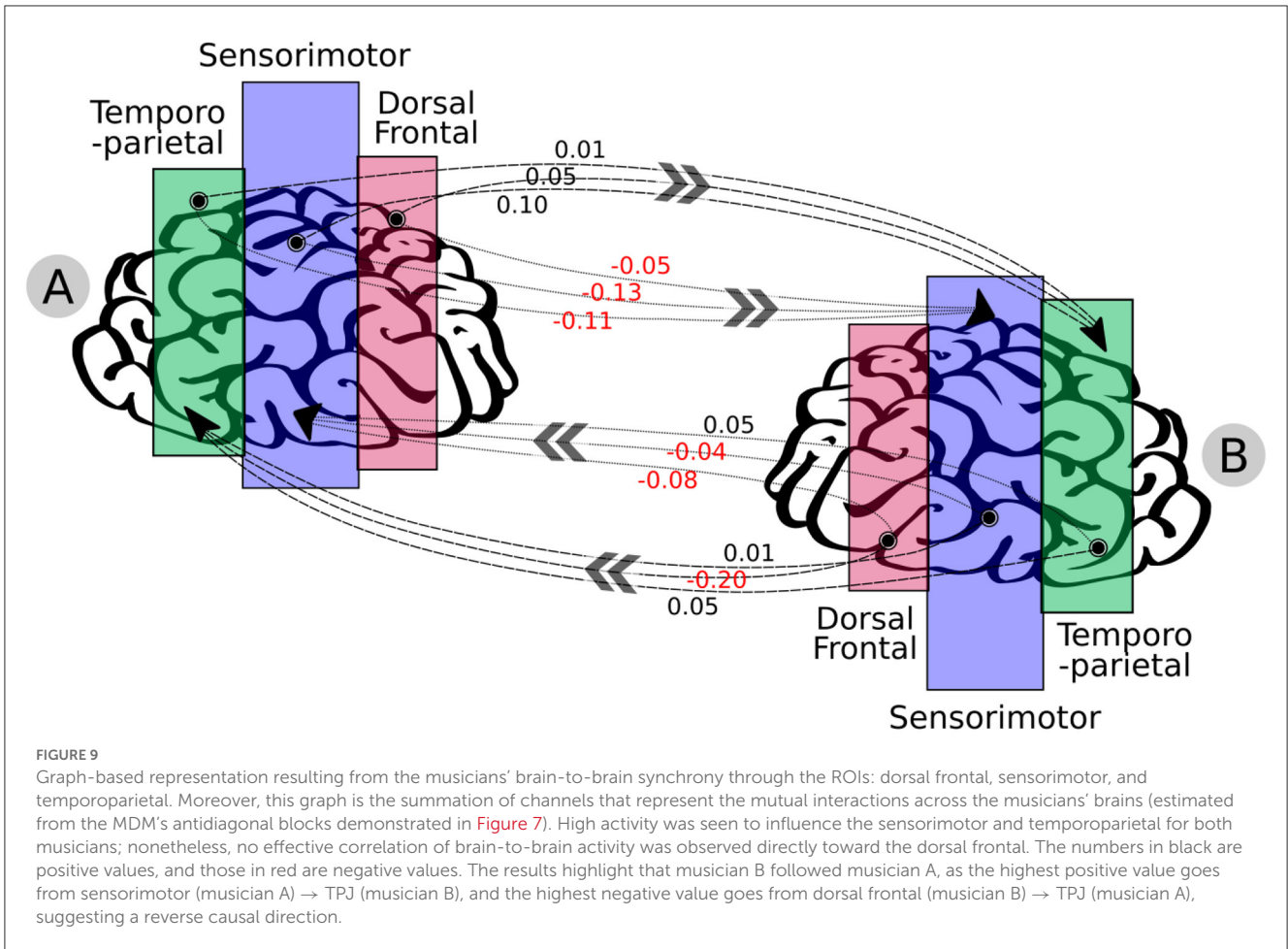
FIGURE 8
ROIs' mean representation, according to the 10-10 EEG montage, of the intra-individuals connectivity as well as the inter-individual based on the MDM-BF.

connectivity (summed through the ROIs' mean according to the 10-10 EEG montage) vs. inter-individual connectivity is represented in Figure 8. The causal direction is from the row to the column, that is, the highest ROI activity from violinist A was from the frontal into the sensorimotor, whereas for violinist B, the causal relation from TPJ into sensorimotor was not strong. Moreover, the strongest observed values across inter-brains were from all three ROIs from violinist A to the TPJ from violinist B (left-bottom picture in the third column).

Broadly speaking, these causal relationships are estimated based on the best-adjusted joint probability distribution between the NIRSout (16 LED light sources leading to 23 time series from each violinist) represented as a network. In the best model, first, the partial DAGs obtained can be said to present the intra- and inter-individual connections, and then, the conditional

independence of the time series is incorporated according to the assumptions of the model. First, the best network structure for each participant is estimated independently, and then, the hyperscanning network structure is also estimated independently from the others. Nonetheless, the three network dynamics cannot be regarded as totally independent because only thetas can show that (if they are zeros). Moreover, a "partializing relationship" can be observed across structures conditioned to the inter-individual vs. intra-individual as the obtained DAGs.

Figure 9 shows the visual representation of the summation of this anti-diagonal block as a graph. For instance, the most influenced regions were sensorimotor and TPJ, as results of the INS, and the results demonstrated that violinist B was influenced by violinist A, as the highest positive value goes from the sensorimotor (violinist A) \rightarrow TPJ (musician B), and the highest negative value goes from



dorsal frontal (violinist B) → TPJ (musician A), suggesting a reverse causal direction.

The uncertainty can be associated with confidence intervals (CI) toward this ROI causal connectivity, which was obtained through the non-parametric bootstrap algorithm (Carpenter and Bithell, 2000), using the MDM average of each posterior. We used the nptest package while considering the mean statistic method, a confidence level of 0.95, and the number of replicates of 50,000 (Table 1). A statistical significance was observed from the dorsal frontal channels' behavior (musician A) → TPJ (musician B), sensorimotor channels' behavior (musician A) → sensorimotor (musician B). In the other direction, it was observed from the dorsal frontal channels' behavior (musician B) → sensorimotor (musician A), dorsal frontal (musician B) → TPJ (musician A), and TPJ (musician B) → TPJ (musician A). The other relations were not statistically significant.

Additionally, by using the MDM class, one can make inferences regarding the time-varying strength of the network's links. For instance, the dynamic change among some channels was noticeable, especially during the resting-stage period (delimited by after the red line), as shown in Figure 10. It is clear that the estimated dynamic of the network links was captured by the MDM.

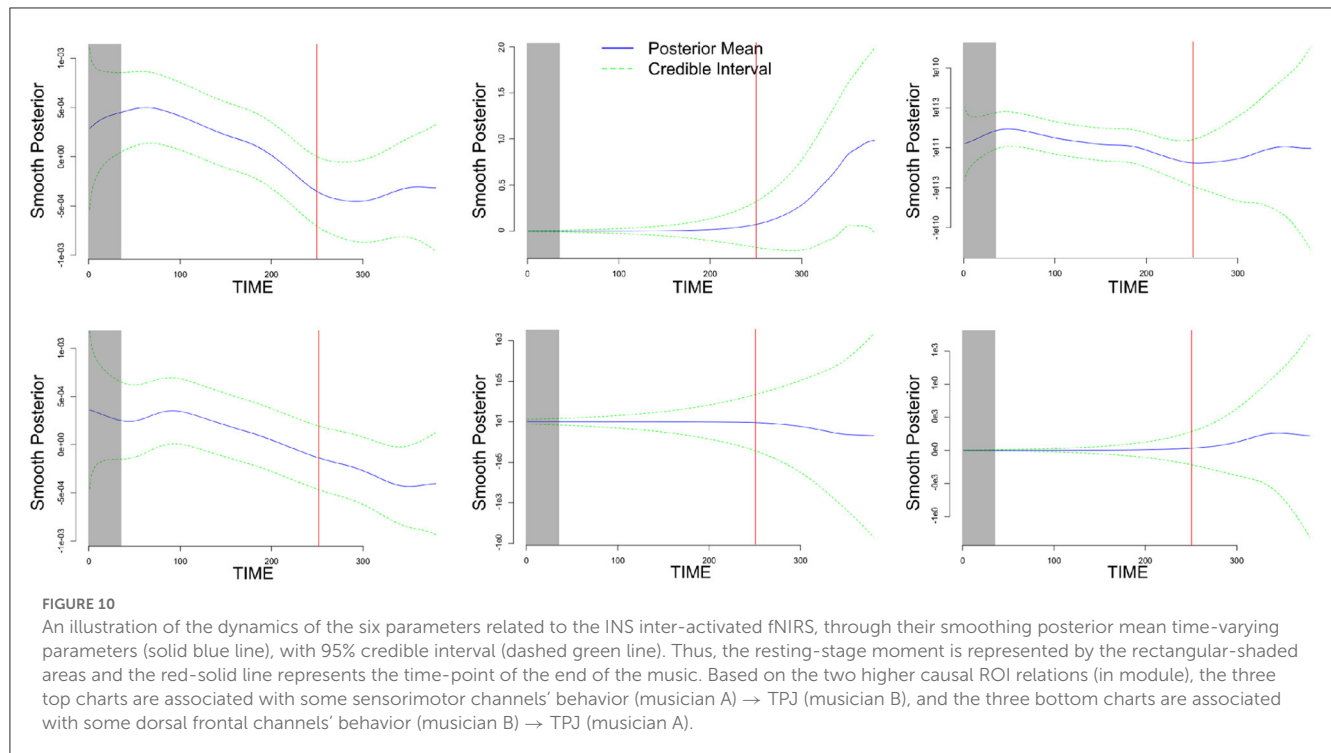
It is clear that intra-subject effective connectivity is stronger than the brain-to-brain coupling strength. Tasks involving music were reported previously and appear to induce brain activation

TABLE 1 Non-parametric bootstrap of the ROIs' mean.

Regions influence	CI 95%	
Frontal_A → TPJ_B	0.00001	0.00581
Sensor_A → Sensor_B	-0.01053	-0.00107
Frontal_B → Sensor_A	-0.00790	-0.00161
Frontal_B → TPJ_A	-0.02136	-0.00311
TPJ_B → TPJ_A	0.00080	0.00422

(Li et al., 2015). Berkowitz and Ansari (2010) discussed the importance of the observed brain region (right TPJ, also called rTPJ) in musicians. Luo et al. (2014) showed neuroimaging toward long-term musical training, which shows an impact on emotional and cognitive function, suggesting the presence of neuroplasticity in the rTPJ.

The sensorimotor and TPJ ROIs presented a greater activation influence from the INS; furthermore, the MDM could capture that musician B was following musician A, which also provides some evidence toward the brain synchronization theory. The hypotheses for the ROIs' inter-individual connections relate to a distinct activation, for instance, highlighted in the literature as resulting from the assessment of different body movements (Kimura, 1977)



or even emotions felt through visual stimuli due to the execution of the activity (Zaitchik et al., 2010).

5. Final remarks

The current study proposes the MDM-BF for fNIRS data obtained in hyperscanning experiments, i.e., simultaneous acquisition, while two or more subjects are interacting. The illustration in a violin duo confirmed the existence of influences of one brain over the other. In the individual brain network analysis for each violinist, it was observed that, although the brain regions work together, some areas play different roles. In other words, some regions connect to others with greater strength. Moreover, this data-driven analysis demonstrated, through their INS estimation, that the influence between violinists is not symmetric and also time-evolving. Therefore, the MDM-BF appears to be a competitive model that is better for hyperscanning studies (due to estimating the effective connectivity) than other methods based on correlation or the consideration of static connections (which only estimate functional connectivity), corroborating similar results that have already been presented in other fields of neuroscience (Costa et al., 2015). In addition, the MDM-BF estimated the inter-brain network using the contemporaneous relationship between regions, without needing to consider the Granger causality.

In the INS analysis [also known as Thinking Through Other Minds (TTOM)], the regions activated on the violinists are represented by the ROI activation and, through the data-driven model, corresponded to the expected results observed in the experimentation (in which musician A was the leader in the duo); that is, the quantification obtained from the MDM-BF brain region connections are highlighted, as shown in Figure 9. However, as this

study considered only a pair of violinists, further studies targeting the brain mapping should be conducted to associate the pattern with more in-depth details regarding those connections. In general, the connections estimated by the MDM-BF for the joint matrix of connections represent the brain ROIs' activity correlations and their dynamic over time, in which all regions present positive meaning and strong connections.

Different for DCM, in this study, social brain network structures could be better explored. The study also analyzed the synchronized dynamical system = globally, as well as the communication of specific parts of the brain. Moreover, the novel procedure for the learning structure network that is presented in this study, or others that are used with the MDM (as the MDM-BF or the MDM-DGM) can be easily applied in other scenarios, such as communication and computer-mediated cooperation games. Furthermore, this approach can be suitable for other neuroscience studies that aim to estimate brain networks and have a large number of nodes. A natural next step will be to incorporate informative priors, in which targets transform the researchers' prior knowledge into hyper-parameters. In addition, parametric space shrinkage should be investigated as an alternative to score-based structure selection. In other words, as a complement to the MDM-BF method, the number of time-varying parameter estimations can be reduced based on some a priori information or some specific criteria.

Data availability statement

The original contributions presented in the study are included in the article/supplementary material, further inquiries can be directed to the corresponding author.

Author contributions

All authors listed have made a substantial, direct, and intellectual contribution to the work and approved it for publication.

Funding

The authors are grateful for the funding partially provided by the Brazilian agencies CNPq, FAPESP, and CAPES. JRSat is grateful to FAPESP (grants 2018/04654-9 and 2018/21934-5).

Conflict of interest

The authors declare that the research was conducted in the absence of any commercial or financial relationships

References

- Babiloni, F., and Astolfi, L. (2014). Social neuroscience and hyperscanning techniques: past, present and future. *Neurosci. Biobehav. Rev.* 44, 76–93. doi: 10.1016/j.neubiorev.2012.07.006
- Baker, J. M., Liu, N., Cui, X., Vrticka, P., Saggat, M., Hosseini, S. H., et al. (2016). Sex differences in neural and behavioral signatures of cooperation revealed by fNIRS hyperscanning. *Sci. Rep.* 6, 26492. doi: 10.1038/srep26492
- Balardin, J. B., Zimeo Morais, G. A., Furucho, R. A., Trambaiolli, L., Vanzella, P., Biazoli, C. Jr., et al. (2017). Imaging brain function with functional near-infrared spectroscopy in unconstrained environments. *Front. Hum. Neurosci.* 11, 258. doi: 10.3389/fnhum.2017.00258
- Balconi, M., and Angioletti, L. (2023). Inter-brain hemodynamic coherence applied to interoceptive attentiveness in hyperscanning: why social framing matters. *Information* 14, 58. doi: 10.3390/info14020058
- Balconi, M., Pezard, L., Nandrino, J.-L., and Vanutelli, M. E. (2017). Two is better than one: the effects of strategic cooperation on intra- and inter-brain connectivity by fNIRS. *PLoS ONE* 12, e0187652. doi: 10.1371/journal.pone.0187652
- Berkowitz, A. L., and Ansari, D. (2010). Expertise-related deactivation of the right temporoparietal junction during musical improvisation. *Neuroimage* 49, 712–719. doi: 10.1016/j.neuroimage.2009.08.042
- Bilek, E., Zeidman, P., Kirsch, P., Tost, H., Meyer-Lindenberg, A., and Friston, K. (2022). Directed coupling in multi-brain networks underlies generalized synchrony during social exchange. *Neuroimage* 252, 119038. doi: 10.1016/j.neuroimage.2022.119038
- Brefczynski-Lewis, J. A., Lutz, A., Schaefer, H. S., Levinson, D. B., and Davidson, R. J. (2007). Neural correlates of attentional expertise in long-term meditation practitioners. *Proc. Nat. Acad. Sci. U. S. A.* 104, 11483–11488. doi: 10.1073/pnas.0606552104
- Brewer, J. A., Worhunsky, P. D., Gray, J. R., Tang, Y.-Y., Weber, J., and Kober, H. (2011). Meditation experience is associated with differences in default mode network activity and connectivity. *Proc. Nat. Acad. Sci. U. S. A.* 108, 20254–20259. doi: 10.1073/pnas.1112029108
- Burger, B., Infantes, G., Ferrané, I., and Lerasle, F. (2009). “DBN versus hmm for gesture recognition in human-robot interaction,” in *International Workshop on Electronics, Control, Modelling, Measurement and Signals (ECMS'09)* (Spain: University of Mondragon), 59–65.
- Carpenter, J., and Bithell, J. (2000). Bootstrap confidence intervals: when, which, what? a practical guide for medical statisticians. *Stat. Med.* 19, 1141–1164. doi: 10.1002/(SICI)1097-0258(20000515)19:9<1141::AID-SIM479>3.0.CO;2-F
- Chen, J., Leong, Y. C., Honey, C. J., Yong, C. H., Norman, K. A., and Hasson, U. (2017). Shared memories reveal shared structure in neural activity across individuals. *Nat. Neurosci.* 20, 115–125. doi: 10.1038/nn.4450
- Chen, L., Qu, Y., Cao, J., Liu, T., Gong, Y., Tian, Z., et al. (2023). The increased inter-brain neural synchronization in prefrontal cortex between simulated patient and acupuncturist during acupuncture stimulation: evidence from functional near-infrared spectroscopy hyperscanning. *Hum. Brain Mapp.* 44, 980–988. doi: 10.1002/hbm.26120
- Chen, M., Zhang, T., Zhang, R., Wang, N., Yin, Q., Li, Y., et al. (2020). Neural alignment during face-to-face spontaneous deception: does gender make a difference? *Hum. Brain Mapp.* 41, 4964–4981. doi: 10.1002/hbm.25173
- Costa, L., Smith, J., Nichols, T., Cussens, J., Duff, E. P., Makin, T. R., et al. (2015). Searching multiregression dynamic models of resting-state fMRI networks using integer programming. *Bayesian Anal.* 10, 441–478. doi: 10.1214/14-BA913
- Cui, X., Bryant, D. M., and Reiss, A. L. (2012). NIRS-based hyperscanning reveals increased interpersonal coherence in superior frontal cortex during cooperation. *Neuroimage* 59, 2430–2437. doi: 10.1016/j.neuroimage.2011.09.003
- Glover, F. (1986). Future paths for integer programming and links to artificial intelligence. *Comp. Operat. Res.* 13, 533–549. doi: 10.1016/0305-0548(86)90048-1
- Gong, G., Rosa-Neto, P., Carbonell, F., Chen, Z. J., He, Y., and Evans, A. C. (2009). Age- and gender-related differences in the cortical anatomical network. *J. Neurosci.* 29, 15684–15693. doi: 10.1523/JNEUROSCI.2308-09.2009
- Hahn, A., Gryglewski, G., Nics, L., Rischka, L., Ganger, S., Sigurdardottir, H., et al. (2018). Task-relevant brain networks identified with simultaneous pet/mr imaging of metabolism and connectivity. *Brain Struct. Funct.* 223, 1369–1378. doi: 10.1007/s00429-017-1558-0
- Hasenkamp, W., and Barsalou, L. W. (2012). Effects of meditation experience on functional connectivity of distributed brain networks. *Front. Hum. Neurosci.* 6, 38. doi: 10.3389/fnhum.2012.00038
- Horwitz, B. (2003). The elusive concept of brain connectivity. *Neuroimage* 19, 466–470. doi: 10.1016/S1053-8119(03)00112-5
- Jiang, L., Stocco, A., Losey, D. M., Abernethy, J. A., Prat, C. S., and Rao, R. P. (2019). Brainnet: a multi-person brain-to-brain interface for direct collaboration between brains. *Sci. Rep.* 9, 1–11. doi: 10.1038/s41598-019-41895-7
- Kimura, D. (1977). Acquisition of a motor skill after left-hemisphere damage. *Brain* 100, 527. doi: 10.1093/brain/100.3.527
- Konvalinka, I., and Roepstorff, A. (2012). The two-brain approach: how can mutually interacting brains teach us something about social interaction? *Front. Hum. Neurosci.* 6, 215. doi: 10.3389/fnhum.2012.00215
- Li, C.-W., Chen, J.-H., and Tsai, C.-G. (2015). Listening to music in a risk-reward context: the roles of the temporoparietal junction and the orbitofrontal/insular cortices in reward-anticipation, reward-gain, and reward-loss. *Brain Res.* 1629, 160–170. doi: 10.1016/j.brainres.2015.10.024
- Li, L., Wang, H., Luo, H., Zhang, X., Zhang, R., and Li, X. (2020). Interpersonal neural synchronization during cooperative behavior of basketball players: a fNIRS-based hyperscanning study. *Front. Hum. Neurosci.* 14, 169. doi: 10.3389/fnhum.2020.00169
- Li, R., Maysless, N., Balters, S., and Reiss, A. L. (2021). Dynamic inter-brain synchrony in real-life inter-personal cooperation: a functional near-infrared spectroscopy hyperscanning study. *Neuroimage* 238, 118263. doi: 10.1016/j.neuroimage.2021.118263

that could be construed as a potential conflict of interest.

Publisher's note

All claims expressed in this article are solely those of the authors and do not necessarily represent those of their affiliated organizations, or those of the publisher, the editors and the reviewers. Any product that may be evaluated in this article, or claim that may be made by its manufacturer, is not guaranteed or endorsed by the publisher.

Author disclaimer

The opinions, hypotheses, conclusions, and recommendations of this study are those of the authors and do not necessarily represent the opinions of the funding agencies.

- Liu, N., Mok, C., Witt, E. E., Pradhan, A. H., Chen, J. E., and Reiss, A. L. (2016). NIRS-based hyperscanning reveals inter-brain neural synchronization during cooperative jenga game with face-to-face communication. *Front. Hum. Neurosci.* 10, 82. doi: 10.3389/fnhum.2016.00082
- Liu, T., and Pelowski, M. (2014). A new research trend in social neuroscience: towards an interactive-brain neuroscience. *PsyCh J.* 3, 177–188. doi: 10.1002/pchj.56
- Liu, T., Saito, G., Lin, C., and Saito, H. (2017). Inter-brain network underlying turn-based cooperation and competition: a hyperscanning study using near-infrared spectroscopy. *Sci. Rep.* 7, 1–12. doi: 10.1038/s41598-017-09226-w
- Luo, C., Tu, S., Peng, Y., Gao, S., Li, J., Dong, L., et al. (2014). Long-term effects of musical training and functional plasticity in salience system. *Neural Plast.* 2014:13. doi: 10.1155/2014/180138
- Morgan, J. K., Santosa, H., Conner, K., Fridley, R., Forbes, E. E., Iyengar, S., et al. (2023). Mother-child neural synchronization is time linked to mother-child positive affective state matching. *Soc. Cogn. Affect. Neurosci.* 18:nsad001. doi: 10.1093/scan/nsad001
- Nagarajan, R., Scutari, M., and Lèbre, S. (2013). *Bayesian Networks in R*. New York, NY: Springer, 125–127.
- Nascimento, D. C., Pinto-Orellana, M. A., Leite, J. P., Edwards, D. J., Louzada, F., and Santos, T. E. (2020). Brainwave nets: are sparse dynamic models susceptible to brain manipulation experimentation? *Front. Syst. Neurosci.* 14, 527757. doi: 10.3389/fnsys.2020.527757
- Nguyen, M., Chang, A., Micciche, E., Meshulam, M., Nastase, S. A., and Hasson, U. (2020). Teacher-student neural coupling during teaching and learning. *bioRxiv*. 40. [preprint] doi: 10.1101/2020.05.07.082958
- Oates, C. J., Costa, L., and Nichols, T. E. (2015). Toward a multisubject analysis of neural connectivity. *Neural Comput.* 27, 151–170. doi: 10.1162/NECO_a_00690
- Palhano-Fontes, F., Barreto, D., Onias, H., Andrade, K. C., Novaes, M. M., Pessoa, J. A., et al. (2019). Rapid antidepressant effects of the psychedelic ayahuasca in treatment-resistant depression: a randomized placebo-controlled trial. *Psychol. Med.* 49, 655–663. doi: 10.1017/S0033291718001356
- Pan, Y., Cheng, X., Zhang, Z., Li, X., and Hu, Y. (2017). Cooperation in lovers: an fNIRS-based hyperscanning study. *Hum. Brain Mapp.* 38, 831–841. doi: 10.1002/hbm.23421
- Pan, Y., Guyon, C., Borrágán, G., Hu, Y., and Peigneux, P. (2021). Interpersonal brain synchronization with instructor compensates for learner's sleep deprivation in interactive learning. *Biochem. Pharmacol.* 191, 114111. doi: 10.1016/j.bcp.2020.114111
- Pearl, J. (2009). *Causality: Models, Reasoning & Inference*. Cambridge: Cambridge University Press.
- Pinto-Orellana, M. A., Nascimento, D. C., Mirtaheiri, P., Jonassen, R., Yazidi, A., and Hammer, H. L. (2020). 1A Hemodynamic Decomposition Model for Detecting Cognitive Load Using Functional Near-Infrared Spectroscopy. *arXiv*. [preprint]. doi: 10.48550/arXiv.2001.08579
- Queen, C. M., and Albers, C. J. (2009). Intervention and causality: forecasting traffic flows using a dynamic bayesian network. *J. Am. Stat. Assoc.* 104, 669–681. doi: 10.1198/jasa.2009.0042
- Queen, C. M., and Smith, J. Q. (1993). Multiregression dynamic models. *J. R. Stat. Soc. Ser. B* 55, 849–870. doi: 10.1111/j.2517-6161.1993.tb01945.x
- R Core Team (2022). *R: A Language and Environment for Statistical Computing*. Vienna: R Foundation for Statistical Computing.
- Reindl, V., Wass, S., Leong, V., Scharke, W., Wistuba, S., Wirth, C. L., et al. (2022). Multimodal hyperscanning reveals that synchrony of body and mind are distinct in mother-child dyads. *Neuroimage* 251, 118982. doi: 10.1016/j.neuroimage.2022.118982
- Scholkmann, F., Holper, L., Wolf, U., and Wolf, M. (2013). A new methodical approach in neuroscience: assessing inter-personal brain coupling using functional near-infrared imaging (fNIRI) hyperscanning. *Front. Hum. Neurosci.* 7, 813. doi: 10.3389/fnhum.2013.00813
- Smith, S. M., Miller, K. L., Salimi-Khorshidi, G., Webster, M., Beckmann, C. F., Nichols, T. E., et al. (2011). Network modelling methods for fMRI. *Neuroimage* 54, 875–891. doi: 10.1016/j.neuroimage.2010.08.063
- Song, M., Zhou, Y., Li, J., Liu, Y., Tian, L., Yu, C., et al. (2008). Brain spontaneous functional connectivity and intelligence. *Neuroimage* 41, 1168–1176. doi: 10.1016/j.neuroimage.2008.02.036
- Van Den Heuvel, M., Mandl, R., and Pol, H. H. (2008). Normalized cut group clustering of resting-state fMRI data. *PLoS ONE* 3, e2001. doi: 10.1371/journal.pone.0002001
- van den Heuvel, M. P., Stam, C. J., Boersma, M., and Pol, H. H. (2008). Small-world and scale-free organization of voxel-based resting-state functional connectivity in the human brain. *Neuroimage* 43, 528–539. doi: 10.1016/j.neuroimage.2008.08.010
- Wang, J., Wang, L., Zang, Y., Yang, H., Tang, H., Gong, Q., et al. (2009). Parcellation-dependent small-world brain functional networks: a resting-state fMRI study. *Hum. Brain Mapp.* 30, 1511–1523. doi: 10.1002/hbm.20623
- Wang, X., Zhang, Y., He, Y., Lu, K., and Hao, N. (2022). Dynamic inter-brain networks correspond with specific communication behaviors: using functional near-infrared spectroscopy hyperscanning during creative and non-creative communication. *Front. Hum. Neurosci.* 16, 907332. doi: 10.3389/fnhum.2022.907332
- Wei, Y., Liu, J., Zhang, T., Su, W., Tang, X., Tang, Y., et al. (2023). Reduced interpersonal neural synchronization in right inferior frontal gyrus during social interaction in participants with clinical high risk of psychosis: an fNIRS-based hyperscanning study. *Progr. Neuropsychopharmacol. Biol. Psychiatry* 120, 110634. doi: 10.1016/j.pnpbp.2022.110634
- West, M., and Harrison, J. (2006). *Bayesian Forecasting and Dynamic Models*. New York, NY: Springer Science & Business Media.
- Zadbood, A., Chen, J., Leong, Y. C., Norman, K. A., and Hasson, U. (2017). How we transmit memories to other brains: constructing shared neural representations via communication. *Cereb. Cortex* 27, 4988–5000. doi: 10.1093/cercor/bhx202
- Zaitchik, D., Walker, C., Miller, S., LaViolette, P., Feczko, E., and Dickerson, B. C. (2010). Mental state attribution and the temporoparietal junction: an fMRI study comparing belief, emotion, and perception. *Neuropsychologia* 48, 2528–2536. doi: 10.1016/j.neuropsychologia.2010.04.031
- Zhang, M., Liu, T., Pelowski, M., Jia, H., and Yu, D. (2017). Social risky decision-making reveals gender differences in the TPJ: a hyperscanning study using functional near-infrared spectroscopy. *Brain Cogn.* 119, 54–63. doi: 10.1016/j.bandc.2017.08.008
- Zhao, H., Li, Y., Wang, X., Kan, Y., Xu, S., and Duan, H. (2022). Inter-brain neural mechanism underlying turn-based interaction under acute stress in women: a hyperscanning study using functional near-infrared spectroscopy. *Soc. Cogn. Affect. Neurosci.* 17, 850–863. doi: 10.1093/scan/nsac005